Countercomplementarity and Strong Ferromagnetic Coupling in a Linear Mixed μ-Acetato, μ-Hydroxo Trinuclear Copper(II) Complex. Synthesis, Structure, Magnetic Properties, EPR, and Theoretical Studies

L. Gutierrez,[†] G. Alzuet,[†] J. A. Real,[†] J. Cano,[†] J. Borrás,*[,†] and A. Castiñeiras[‡]

Departamento de Química Inorgánica, Universidad de Valencia, Avda Vicent Estellés s/n, 46100-Burjassot, Spain, and Departamento de Química Inorgánica, Facultad de Farmacia, Universidad de Santiago, 15703-Santiago de Compostela, Spain

Received February 28, 2000

The structural and magnetic data of the trinuclear compound $[Cu_3(L)_2(CH_3COO)_2(OH)_2(dmf)_2]$ (HL = *N*-(2-methylpyridyl)toluensulfonylamide) are reported. The compound crystallizes in the monoclinic system, space group $P2(1)/n$ (no. 14), with $a = 11.6482(6)$ Å, $b = 13.5772(6)$ Å, $c = 13.5306(7)$ Å, $\alpha = 90°$, $\beta = 92.859(5)°$, $\gamma = 90°$, and $Z = 2$. The three copper atoms form an exact linear arrangement. Neighboring coppers are connected by a hydroxo bridge and a bidentate *syn*−*syn* carboxylato group. The coordination spheres of the terminal copper atoms are square pyramidal with a dmf molecule as the apical ligand. The central copper has a regular square planar geometry. The mixed bridging by a hydroxide oxygen atom and a bidentate carboxylato group leads to a noncoplanarity of the adjacent basal coordination planes with a dihedral angle of 51.96(9)°. Susceptibility measurements (2−300 K) reveal a strong ferromagnetic coupling, $J = 93(6)$ cm^{-1}, in the mixed-bridged moiety leading to a quartet ground state that is confirmed by the EPR spectra. The ferromagnetic exchange coupling is discussed using DFT calculations on model compounds that have shown a countercomplementary effect of the hydroxo and acetate bridges.

Introduction

Current research work concerning the structural and magnetic properties of polynuclear transition-metal compounds is aimed at understanding the structural and chemical features governing electronic exchange coupling through multiatom bridging ligands. Although the greatest effort and success have been in the study of dinuclear copper(II) complexes, there has been little work on oligomeric copper(II) complexes with more than two copper ions, particularly on linear trinuclear compounds primarily due to a lack of suitably characterized compounds. The molecular structures of trinuclear copper complexes reveal three kinds of clusters consisting of triangular arrays (isosceles or equilateral) and strictly linearly arranged copper ions. The magnetic behavior of these complexes may be antiferromagnetic or ferromagnetic.[1] The former leads to a doublet ground state and the latter to a quartet ground state, which is uncommon within trinuclear copper(II) complexes investigated so far. Linear trinuclear Cu(II) compounds are relatively rare, and only a few are studied magnetically.[2]

Several synthetic approaches have been proposed to design discrete polynuclear complexes. One of them consists of the introduction of bidentate or tridentate terminal ligands[3] and multiatom bridging ligands such 3,4,5-substituted triazoles[4] or carboxylato groups.[5] Another consists of the use of compartmental ligands, which are organic molecules able to hold together two or more metal ions.[6]

In this paper we focus on the linear trinuclear complex $[Cu_3(L)_2(CH_3COO)_2(OH)_2(dmf)_2]$, which is derived from the bidentate ligand *N*-(2-methylpyridyl)toluensulfonylamide (HL) (Chart 1). Compared with the ubiquitous chemistry of amine-based ligands, the coordination chemistry of the sulfonamide derivatives ($R^1-NH-SO_2-R^2$) is much less well developed. In fact, although there are many areas of considerable potential interest for sulfonamide coordination chemistry, this area is relatively unexplored.[7] We have studied the behavior as ligands of several sulfonamides (e.g., acetazolamide, methazolamide)[8] and sulfonamide *N*-derivatives such as sulfathiazole or sulfacetamide.[9] In general, these ligands require deprotonation of the sulfonamido group to delocalize the negative charge through the R groups that promotes the bond with the metal ion. We have obtained only a few examples of polynuclear metal

* To whom correspondence may be addressed. Phone: (+34)-96-3864530. Fax: (+34)-96-3864960. E-mail: Joaquin.Borras@uv.es.
[†] Universidad de Valencia.
[‡] Universidad de Santiago.

(1) Chaudhuri, P.; Winter, M.; Della Védova, B. P. C.; Bill, E.; Trautwein, A.; Gehring, S.; Fleischhauer, P.; Nuber, B.; Weiss, J. *Inorg. Chem.* **1991**, *30*, 2148.
(2) van Albada, G. A.; Mutikainen, I.; Turpeinen, U.; Reedijk, J. *Eur. J. Inorg. Chem.* **1998**, 547.
(3) Costa, R.; García, A.; Ribas, J.; Mallah, T.; Journaux, Y.; Sletten, J.; Xolans, X.; Rodríguez, V. *Inorg. Chem.* **1993**, *32*, 3733.
(4) (a) Prins, R.; Biagini-Cingi, M.; Drillon, M.; de Graaff, R. A. G.; Haasnoot, J.; Manotti-Lanfredi, A. M.; Rabu, P.; Reedijk, J.; Ugozzoli, F. *Inorg. Chim. Acta* **1996**, *248*, 35. (b) Liu, J.; Song, Y.; Yu, Z.; Zhuang, J.; Huang, X.; You, X. *Polyhedron* **1999**, *18*, 1491. (c) Liu, J. C.; Fu, D. G.; Zhuang, J. Z.; Duan, C. Y.; You, X. Z. *J. Chem. Soc., Dalton Trans*. **1999**, 2337.
(5) Colacio, E.; Dominguez-Vera, J. M.; Kivekas, R.; Moreno, J. M.; Romerosa, A.; Ruiz, J. *Inorg. Chim. Acta* **1993**, *212*, 115.
(6) (a) Chen, X.; Zhan, S.; Hu, C.; Meng, Q.; Liu, Y. *J. Chem. Soc., Dalton Trans.* **1997**, 245. (b) Tuna, F.; Patron, L.; Journaux, Y.; Andruh, M.; Plass, W.; Trombe, J. C. *J. Chem. Soc., Dalton Trans.* **1999**, 539.
(7) Otter, C. A.; Couchman, S. M.; Jeffery, J. C.; Mann, K. L. V.; Psillakis, E.; Ward, M. *Inorg. Chim. Acta* **1998**, *278*, 178.
(8) (a) Ferrer, S.; Borrás, J.; Miratvilles, C.; Fuertes, A. *Inorg. Chem.* **1990**, *29*, 206. (b). Alzuet, G.; Ferrer, S.; Borrás, J.; Solans, X.; Font-Bardía, M. *Inorg. Chim. Acta* **1993**, *203*, 257.
(9) (a) Casanova, J.; Alzuet, G.; LaTorre, J.; Borrás, J. *Inorg. Chem.* **1997**, *36*, 2052 (b) Blasco, F.; Perelló, L.; LaTorre, J.; Borrás, J.; García-Granda, S. *J. Inorg. Biochem*. **1996**, *61*, 143.

10.1021/ic000218m CCC: $19.00 © 2000 American Chemical Society
Published on Web 07/21/2000

Chart 1. *N*-(2-methylpyridyl)toluenesulfonylamide

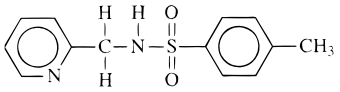

complexes with this type of ligand, and in all the cases the sulfonamide moiety is the bridging ligand.[8a,9a]

The compound reported here is one of the scarce examples of a trinuclear complex with both μ-hydroxo and μ-acetato anions that presents a strong ferromagnetic behavior. This ferromagnetism stems from the noncomplementarity nature of the magnetic exchange through these ligands. A similar situation has been found by Haase et al.[10] in the system [bis(μ-benzoato-*O*,*O*′)bis(benzoato-*O*)bis(μ-(2-diethylamino)ethanolato-*O*,*N*)]bis-(methanol)tricopper(II), which is the only ferromagnetic linear trinuclear copper(II) complex fully characterized up to now.

Experimental Section

***N*-(2-methylpyridyl)toluensulfonylamide (HL).** 2-Picolylamine (1.081 g, 10.0 mmol) (Sigma Chemical) was added to an aqueous solution of NaOH (0.4 g, 10.0 mmol). To this solution was added a solution of *p*-toluensulfonyl chloride (Sigma Chemical) (1.9 g, 10.0 mmol) in THF (20 mL) slowly with stirring. After the resulting mixture was stirred for 4 h, the THF solvent was removed at 60 °C under reduced pressure. The white solid obtained was then dissolved in 20 mL of hot EtOH. This solution was left to cool at room temperature, and white crystals were obtained. HL yield: 67%. Anal. Calcd for $C_{13}H_{14}N_2O_2S$ (262): C, 59.5; H, 5.3; N, 10.7; S, 12.2. Found: C, 58.8; H, 5.5; N, 10.2; S, 11.5. IR (KBr) (cm^{-1}): 3113 ν(N−H); 1329, 1164 $\nu(SO_2)$; 818 ν(S−N).

Bis(μ-acetato)bis(μ-hydroxo)bis(*N*-(2-methylpyridyl)toluensulfonylamidate)tricopper(II)·2dmf. The copper complex was prepared by the reaction of the metal acetate (1 mmol in 25 mL of dmf) with the ligand (1 mmol in 25 mL of dmf). Slow evaporation of the resulting solution at room temperature provided blue crystals of the title compound suitable for X-ray diffraction. Microanalysis of the dried crystals was satisfactory. Anal. Calcd for $C_{34}H_{52}Cu_3N_6O_{10}S_2$ (1011.54): C, 42.55; H, 5.46; N, 8.76; S, 6.68. Found: C, 42.91; H, 4.82; N, 8.34; S, 6.41. IR(KBr) (cm^{-1}): 3499 ν(O−H); 1590 ν_{as}(COO); 1430 ν_s(COO); 1271, 1139 $\nu(SO_2)$; 954 ν(S−N). Diffuse reflectance (λ_{max}): 15260 cm^{-1}. UV−vis (dichloromethane) (λ_{max}): 15 260 cm^{-1}. FAB MS: *m*/*z* 1034 [M^+].

X-ray Structure Determination. A blue prismatic crystal of $[Cu_3(L)_2(CH_3COO)_2(OH)_2(dmf)_2]$ was mounted onto a glass fiber and used for data collection. Cell constants and an orientation matrix for data collection were obtained by least-squares refinement of the diffraction data from 25 reflections in the range of $21.402° < \theta < 45.461°$ in an Enraf Nonius CAD4 automatic diffractometer.[11] Data were collected at 293 K using Cu Kα radiation (λ = 1.541 84 Å) and the ω-scan technique, and corrected for Lorentz and polarization effects.[12] A semiempirical absorption correction (σ scan) was made.[13] The structure was solved by direct methods[14] and subsequent difference Fourier maps, and refined on F^2 by a full-matrix least-squares procedure using anisotropic displacement parameters.[15] All hydrogen atoms were located in their calculated positions (C−H 0.93−0.97 Å) except those of the pyridine and OH, which were located from difference Fourier maps. The located H atoms were refined isotropically, whereas the calculated H atoms were refined using a riding model. The C and O atoms of the dmf molecule are disordered over two positions; the occupancy factor for each was refined, resulting in values of 0.30 (C30A), 0.70 (O30B), 0.54 (C31A), 0.46 (C31B), 0.51 (C32A), 0.49 (C32B), 0.59 (C33A), and 0.41 (C33B). Atomic scattering factors are from the *International Tables for X-ray Crystallography*.[16] Molecular graphics are from ZORTEP.[17] A summary of the crystal data, experimental details, and refinement results are listed in Table 1. Atomic coordinates and equivalent isotropic displacement parameters are collected in Table 2.

Table 1. Crystal Data and Structure Refinement for $[Cu_3(L)_2(CH_3COO)_2(OH)_2(dmf)_2]$

empirical formula	$C_{36}H_{48}Cu_3N_6O_{12}S_2$	*Z*	2
fw	1011.54	λ, Å	1.54184
space group	*P*2(1)/*n* (no. 14)	μ_{calcd}, cm^{-1}	32.10
a, Å	11.6482(6)	ρ_{calcd}, $g\cdot cm^{-3}$	1.572
b, Å	13.5772(6)	*T*, K	293(2)
c, Å	13.5306(7)	R^a	0.0418
β, (deg)	92.859(5)	$R_w{}^b$	0.1156
V, $Å^3$	2137.20(18)		

[a] $R = \sum||F_o| - |F_c||/\sum|F_o|$. [b] $R_w = \{\sum[w(F_o^2 - F_c^2)^2]/\sum[w(F_o^2)^2]\}^{1/2}$.

Table 2. Atomic Coordinates ($\times 10^4$) and Equivalent Isotropic Displacement Parameters ($Å^2 \times 10^3$) for $[Cu_3(L)_2(CH_3COO)_2(OH)_2(dmf)_2]$

	x	*y*	*z*	*U*(eq)[a]
Cu(1)	3467(1)	1367(1)	6337(1)	42(1)
Cu(2)	5000	0	5000	44(1)
S(1)	5435(1)	2914(1)	7137(1)	46(1)
O(1)	4515(2)	1295(2)	5317(2)	49(1)
O(11)	5893(2)	2766(2)	6175(2)	58(1)
O(12)	5467(2)	3907(2)	7518(2)	61(1)
O(21)	2339(2)	569(2)	5541(2)	51(1)
O(22)	3415(2)	−410(2)	4633(2)	56(1)
O(30)	4419(4)	−215(3)	6897(4)	123(2)
N(1)	2277(2)	1490(2)	7351(2)	43(1)
N(2)	4179(2)	2471(2)	7127(2)	47(1)
N(31)	5317(3)	−1106(3)	8078(3)	75(1)
C(1)	1307(3)	948(3)	7377(3)	52(1)
C(2)	510(3)	1092(3)	8072(3)	58(1)
C(3)	709(3)	1816(3)	8773(3)	59(1)
C(4)	1697(3)	2359(3)	8765(3)	56(1)
C(5)	2468(3)	2181(2)	8041(2)	45(1)
C(6)	3573(3)	2741(3)	8003(3)	64(1)
C(7)	6297(3)	2208(2)	7987(2)	45(1)
C(8)	6730(3)	1307(3)	7694(3)	51(1)
C(9)	7380(3)	747(3)	8356(3)	58(1)
C(10)	7621(3)	1049(3)	9316(3)	58(1)
C(11)	7186(4)	1951(3)	9598(3)	68(1)
C(12)	6531(3)	2534(3)	8944(3)	59(1)
C(13)	8316(4)	421(4)	10040(4)	84(1)
C(20)	2475(3)	−88(2)	4905(2)	43(1)
C(21)	1410(3)	−542(3)	4426(3)	58(1)
C(31A)	4565(10)	−503(9)	7783(9)	92(4)
C(31B)	5161(8)	−825(7)	7171(7)	65(3)
C(32A)	6148(8)	−1539(8)	7363(10)	100(4)
C(32B)	4562(16)	−495(15)	8745(12)	167(9)
C(33)	5797(11)	−1633(8)	8807(9)	267(8)

[a] *U*(eq) is defined as one-third of the trace of the orthogonalized U_{ij} tensor.

Physical Methods. The variable temperature magnetic susceptibility measurements were carried out on a microcrystalline sample (4 mg) using a Quantum Design MPMS2 SQUID susceptometer equipped with a 55 kG magnet and operating at 10 kG in the range of 1.8−400 K. The susceptometer was calibrated with $(NH_4)_2Mn(SO_4)_2\cdot 12H_2O$. The corrections for the diamagnetism were estimated from Pascal constants. The infrared spectra (ν = 400−4000 cm^{-1}) were obtained on a Mattson Satellite FTIR spectrophotometer. Elemental analyses were performed

(10) (a) Haase, W.; Gehring, S. *J. Chem. Soc., Dalton Trans*. **1985**, 2609. (b) Ghering, S.; Haase, W.; Paulus, H. *Acta Crystallogr*. **1991**, *C47*, 1814. (c) Fleischhauer, P.; Gehring, S.; Haase, W. *Ber. Bunsen-Ges. Phys. Chem.* **1992**, *96*, 1701. (d) Gehring, S.; Fleischhauer, P.; Paulus, H.; Haase, W. *Inorg. Chem.* **1993**, *32*, 54. (e) Fleischhauer, P.; Gehring, S.; Saal, C.; Haase, W.; Tomkowicz, Z.; Zanchini, C.; Gatteschi, D.; Davidof, D.; Barra, A. L. *J. Magn. Magn. Mater.* **1996**, *159*, 166.
(11) Nonius, B. V. CAD4-Express Software, Ver. 5.1/1.2, Enraf Nonius, Delft, The Netherlands, 1994.
(12) Kretschmar, M. GENHKL Program for the reduction of CAD4, 1997.
(13) North, A. C. T.; Phillips, D. C.; Mathews, F. S. *Acta Crystallogr*. **1968**, *A24*, 351.
(14) Sheldrick, G. M. *Acta Crystallogr*. **1990**, *A46*, 467−473.
(15) Sheldrick, G. M. SHELXL-97. Program for the Refinement of Crystal Structures, University of Goettingen, Germany, 1997.
(16) *International Tables for X-ray Crystallography*; Kluwer Academic Publishers: Dordrecht, The Netherlands, 1995; Vol. C.
(17) Zoslnai, L. ZORTEP. A program for the Presentation of Thermal Ellipsoids, University of Heidelberg, Germany, 1997.

by a Carlo Erba AAS instrument. Diffuse reflectance and UV−vis spectra was recorded on a Shidmazu 2101 PC spectrophotometer. EPR spectra of ground crystals were carried out at X-band with a Bruker ER200D equipped with an Oxford continuous flow cryostat.

Computational Details. A detailed description of the computational strategy adopted in this work has been described elsewhere[18] and is only briefly reviewed here. For the evaluation of the coupling constant of dinuclear models, two separate calculations are carried out by means of density functional theory,[19] one for the triplet state and another for the singlet state. For the trinuclear compound, three calculations are necessary, one for the quadruplet and one for each one of two doublets. The hybrid B3LYP method,[20] as implemented in Gaussian-98,[21] has been used in all calculations, mixing the exact Hartree−Fock exchange with Becke's expression for the exchange[22]and with the Lee−Yang−Parr correlation functional.[23] Double-ζ quality and triple-ζ quality basis sets proposed by Ahlrichs[24] have been employed for nonmetallic and metallic atoms, respectively. The presence of a low-energy singlet (for dinuclear models) or doublet (for trinuclear models) makes it difficult to evaluate accurately the energy of the lowest singlet or doublet by a single-determinant method. To solve this problem, broken-symmetry wave functions, as proposed by Noodlemann et al., have been used.[25−28] One of us has found previously that, among the most common functionals, the B3LYP method combined with the broken-symmetry treatment is the strategy which provides the best results for calculating coupling constants.[20−32] It is clear that for broken-symmetry Hartree−Fock calculations it is necessary to make a correction due to the multideterminant character of the wave function of the low-multiplicity state.[30] On the other hand, for DTF calculations we adopt single-determinant wave functions for which the DTF is well defined.[33−35] Then, we use the broken-symmetry energy calculated by DTF methods as the real energy of the state.

For this system (see Chart 2a), the spin Hamiltonian describing the low-lying states in the absence of a magnetic field may be written as

$$\mathbf{H} = -J(\mathbf{S_1S_2} + \mathbf{S_2S_3}) - J'\mathbf{S_1S_3} \qquad (1)$$

where J and J' are the exchange coupling constants between the neighboring and nonneighboring centers, respectively. The local anisotropies and anisotropic interactions have not been considered. Applying the Hamiltonian to the nonpure spin functions, we make the energy matrix. By diagonalization of this matrix, we obtain the energy as a function of J and J' constants for the three possible states (one quadruplet and two doublets).[36] The energies of the quadruplet (Q) and the doublet (D_1 and D_2) states and, considering $\alpha = J/J'$, the pure spin functions of the microstate $|M_s,S_i\rangle$ are (the subscript denotes the state)

Chart 2. Spin Diagram for $[Cu_3(L)_2(CH_3COO)_2(OH)_2(dmf)_2]$

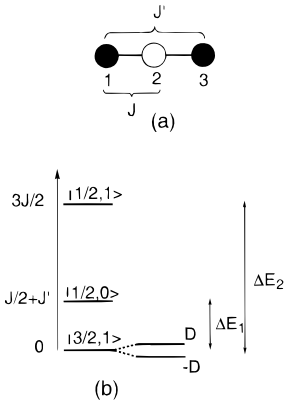

$$E_Q = -J/2, \quad E_{D_1} = J', \quad E_{D_2} = J$$

$$|3/2,3/2_Q\rangle = |\alpha\alpha\alpha\rangle$$

$$|-3/2,3/2_Q\rangle = |\beta\beta\beta\rangle$$

$$|1/2,3/2_Q\rangle = (1/2)^{1/2}|\alpha\alpha\beta\rangle - (1/2)^{1/2}|\beta\alpha\alpha\rangle$$

$$|-1/2,3/2_Q\rangle = (1/2)^{1/2}|\beta\beta\alpha\rangle - (1/2)^{1/2}|\alpha\beta\beta\rangle$$

$$|1/2,1/2_{D_1}\rangle = c_1|\alpha\alpha\beta\rangle + c_2|\alpha\beta\alpha\rangle + c_1|\beta\alpha\alpha\rangle$$

$$|-1/2,1/2_{D_1}\rangle = c_1|\beta\beta\alpha\rangle + c_2|\beta\alpha\beta\rangle + c_1|\alpha\beta\beta\rangle$$

$$|1/2,1/2_{D_2}\rangle = c_3|\alpha\alpha\beta\rangle - c_4|\alpha\beta\alpha\rangle + c_3|\beta\alpha\alpha\rangle$$

$$|-1/2,1/2_{D_2}\rangle = c_3|\beta\beta\alpha\rangle - c_4|\beta\alpha\beta\rangle + c_3|\alpha\beta\beta\rangle$$

$$c_1 = 0.57735 + 0.33601\alpha + 0.10199\alpha^2/1 + 0.47230\alpha + 0.14413\alpha^2$$

$$c_2 = 0.57735 + 0.13545\alpha/1 + 0.452665\alpha + 0.098845\alpha^2$$

$$c_3 = 0.40825 + 0.095782\alpha/1 + 0.452665\alpha + 0.098845\alpha^2$$

$$c_4 = 0.81650 + 0.47511\alpha + 0.14404\alpha^2/1 + 0.47230\alpha + 0.14413\alpha^2$$

For any value, the main contribution to the wave function of the microstate of the state D_1 is given by the nonpure spin function $|\alpha\alpha\beta\rangle$. We use this broken-symmetry (BS) or nonpure spin function to calculate the energy of the state D_1. In the same way, the $|\alpha\beta\alpha\rangle$ BS function provides us the energy of the doublet D_2. Finally, the energy of the quadruplet state is estimated by DFT calculation on the configuration $|\alpha\alpha\alpha\rangle$.

The J and J' values are calculated using the calculated broken-symmetry energies by DFT methods:

$$J = 2/3(E_{D_1} - E_Q) \qquad (2)$$

$$J' = (E_{D_2} - E_{D_1}) + J \qquad (3)$$

Results and Discussion

Crystal Structure. The trinuclear entity with the atomic labeling scheme used is shown in Figure 1. Bond distances and angles are collected in Table 3. The complex molecule consists of a neutral symmetrical trinuclear unit and two disordered dimethylformamide molecules, the Cu(2) being the center of symmetry. The terminal copper atoms Cu(1) and Cu(1A) have a distorted square pyramidal geometry ($\tau = 0.22$) coordinated by two nitrogen atoms, N(1) and N(2) of the pyridyl ring and of the sulfonamidato group of the deprotonated ligand (L), the

(18) Ruiz, E.; Alemany, P.; Alvarez, S.; Cano, J. *J. Am. Chem. Soc.* **1997**, *119*, 1927.
(19) Parr, R. G.; Yang, W. *Density-Functional Theory of Atoms and Molecules*; Oxford University Press: New York 1989.
(20) Becke, A. D. *J. Chem. Phys.* **1993**, *98*, 5648.
(21) Frisch, M. J.; Pople, J. A. Gaussian, Pittsburgh, PA, 1999.
(22) Becke, A. D. *Phys. Rev.* **1988**, *A38*, 3098.
(23) Lee, C.; Yang, W.; Parr, R. G. *Phys. Rev.* **1988**, *B37*, 785.
(24) Schafer, A.; Horn, H.; Ahlrichs, R. *J. Chem. Phys.* **1992**, *97*, 2571.
(25) Noodlemann, L.; Peng, C. Y.; Case, D. A.; Mouesca, J. M. *Coord. Chem. Rev.* **1995**, *144*, 199.
(26) Noodlemann, L.; Case, D. A. *Adv. Inorg. Chem.* **1992**, *38*, 423.
(27) Noodlemann, L.; Davidson, E. R. *Chem. Phys.* **1986**, *109*, 131.
(28) Noodlemann, L. *J. Chem. Phys.* **1981**, *74*, 5737.
(29) Cano, J.; Ruiz, E.; Alemany, P.; Lloret, F.; Alvarez, S. *J. Chem. Soc., Dalton Trans.* **1999**, 1669.
(30) Ruiz, E.; Cano, J.; Alvarez, S.; Alemany, P. *J. Comput. Chem.* **1999**, *20*, 1391.
(31) Cano, J.; Alemany, P.; Alvarez, S.; Verdaguer, M.; Ruiz, E. *Chem. Eur. J.* **1998**, *4*, 476.
(32) Ruiz, E.; Cano, J.; Alvarez, S.; Alemany, P. *J. Am. Chem. Soc.* **1998**, *120*, 11122.
(33) Perdew, J. P.; Savin, A.; Burke, K. *Phys. Rev. A* **1995**, *51*, 4531.
(34) Miehlich, B.; Stoll, H.; Savin, A. *Mol. Phys.* **1997**, *91*, 527.
(35) Goursot, A.; Malrieu, J. P.; Salahub, D. R. *Theor. Chim. Acta* **1995**, *91*, 225.
(36) Kahn, O. *Molecular Magnetism*; VCH: New York, 1993.

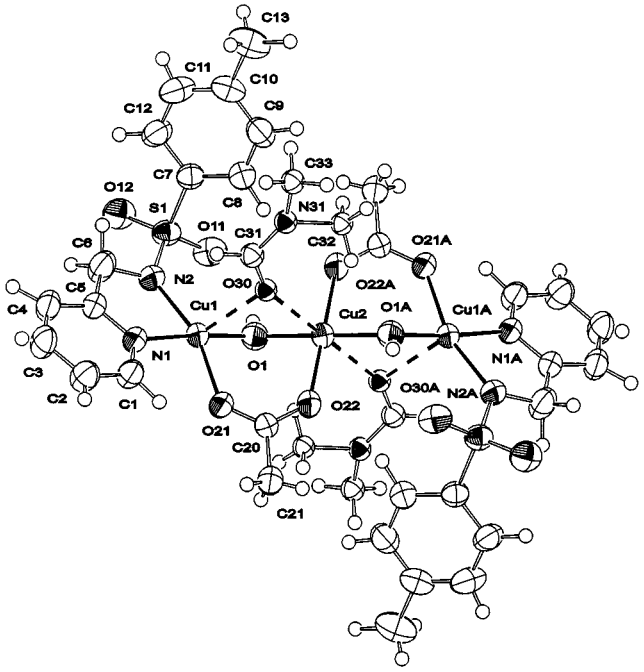

Figure 1. Molecular structure of $[Cu_3(L)_2(CH_3COO)_2(OH)_2(dmf)_2]$ showing the atom numbering scheme. Thermal ellipsoids are drawn at the 50% probability level.

O(1) of the hydroxo bridge, the O(21) of the acetate bridge, and one O(30) from a dimethylformamide solvent molecule. For the central Cu(2) a regular square plane geometry is realized with the O(1), O(1A), O(22), and O(22A) atoms from the hydroxo and acetate bridging groups, respectively. The two O(30) and O(30A) atoms from the dimethylformamide (dmf) molecules linked to the Cu(1) and Cu(1A) centers are near the Cu(2) at about 3 Å.

Adjacent copper centers are bridged by the oxygen atom of the hydroxo ligand [Cu(1)−O(1)−Cu(2) = 114.96(12)°] and two oxygen atoms of a bidentate *syn*−*syn* carboxylato group, O(21)−C(22)−O(22), leading to a mixed-bridged coplanar coordination geometry with Cu(1)−Cu(2) = 3.1983(4) Å. The Cu(2)−O(1) and Cu(2)−O(22) bond distances are 1.902(2) and 1.968(2) Å, respectively. The Cu(1)−N(1) and Cu(1)−N(2) lengths are 2.005(3) and 1.997(3) Å, respectively, and the Cu(1)−O(1) and Cu(1)−O(21) bond distances are 1.891(2) and 1.980(2) Å. The apical bond distance Cu(1)−O(30) is 2.517(4) Å. The Cu(1) atom is 0.1628 Å up to the square plane formed by the N(1), N(2), O(1), and O(21) atoms. The Cu(1A) is 0.1628 Å down to the square plane formed by the N(1A), N(2A), O(1A), and O(21A) atoms. The skeleton Cu(1A)−O(1)−Cu(2)−O(1A)−Cu(1) is in a zigzag arrangement, with the three copper ions forming a straight line with an angle of 180°. The mixed bridging leads to a noncoplanarity of the basal N(1)N(2)O(1)O(2) and O(1)O(22)O(22A)O(21A) planes characterized by a folding angle of 51.96(9)°.

IR and Electronic Spectrum. The IR spectrum of the trinuclear copper complex shows a band at 3499 cm^{-1} characteristic of the O−H bridging group.[37] The ν(N−H) vibration of the sulfonamido group of the ligand is absent in the complex, which is in good agreement with the deprotonation of the sulfonamide ligand. The characteristic vibrations of the acetato group in the spectrum confirm that it acts as a bridging bidentate ($\Delta\nu = \nu_{as}(COO) - \nu_s - (COO) = 160$ cm^{-1}).[38] As a consequence of the deprotonation and coordination of the sulfonamido N, the characteristic bands of the SO_2 group are shifted from 1329 and 1164 cm^{-1} in HL to 1271 and 1139 cm^{-1} in the complex. The new band in the spectrum of the complex at 1665 cm^{-1} is assigned to the ν(C═O) vibration of the dimethylformamide.

Both reflectance and dichloromethane solution spectra of the trinuclear complex show a broad weak band centered at about 15260 cm^{-1}. This band must include those corresponding to the two CuN_2O_2 and CuO_4 chromophores present in the compound, which appear at about 16 000 and 13 000 cm^{-1}, respectively.[39]

The FAB mass spectrum of dichloromethane solutions displayed parent peaks centered at *m*/*z* 1036 $[Cu_3(L)_2(CH_3COO)_2(OH)_2{\cdot}2(dichloromethane)(H^+)_2]$, indicating that, at least, the trinuclear core is present in dichloromethane solution.

Magnetic Properties. The temperature dependence of the $\chi_M T$ product for $[Cu_3(L)_2(CH_3COO)_2(OH)_2(dmf)_2]$ (χ_M being the magnetic susceptibility per trimer unit and T the absolute temperature) in the temperature range 2−300 K is shown in Figure 2. At room temperature $\chi_M T$ is 1.33 cm^3 mol^{-1} K, a value which is somewhat larger than that expected for a magnetically uncoupled trinuclear Cu(II) compound (1.23 cm^3 mol^{-1} K for $g = 2.1$). Upon cooling of the sample, $\chi_M T$ increases and reaches a value of 1.95 cm^3 mol^{-1} K in the 6−15 K temperature range. This behavior is indicative of strong ferromagnetic coupling between the adjacent Cu(II) in the trinuclear species. Below 5 K, $\chi_M T$ decreases rapidly down to 1.71 cm^3 mol^{-1} K, which is most likely due to zero-field splitting (ZFS) within the quartet ground state. The occurrence of intermolecular antiferromagnetic interactions may also be operative at very low temperatures.

The X-ray crystal structure of the compound has shown that the three copper(II) ions lie on the same straight line in the arrangement shown in Figure 1. The spin Hamiltonian appropriate to describe the exchange interaction in a linear symmetric trimer has the form

$$\mathbf{H} = -J(\mathbf{S_1S_2} + \mathbf{S_2S_3}) - J'\mathbf{S_1S_3} + D[\mathbf{S_z}^2 - S(S+1)/3] + g\beta H\mathbf{S} \quad (4)$$

where we have included the occurrence of axial ZFS between the ±3/2 and ±1/2 Kramers doublets arising from the $S = 3/2$ ground state. The exchange parameters J and J' refer to the interaction between two adjacent centers and the interaction between the terminal centers, respectively. The resulting spin multiplets are two doublets ($S = 1/2$) and one quartet ($S = 3/2$).[40a] D denotes the half energy gap between the above-mentioned Kramers doublets. The energies of the three spin states are shown in Chart 2.

To reduce the number of parameters, in the first step we have set $D = 0$ in expression 4. In this particular case, the fitting of the experimental data for $T > 10$ K to Hamiltonian 4 confirms that the values of J and J' are strongly correlated in determining the temperature dependence of the magnetic susceptibility as already has been observed for other similar systems.[40b] In fact, we obtain good fits with almost superimposable calculated $\chi_M T$

(37) Christou, G.; Perlepes, S. P.; Libby, E.; Foltong, K.; Huffman, J. C.; Webb, R. J.; Hendrickson, D. N. *Inorg. Chem.* **1990**, *29*, 3657.

(38) Deacon, G. G. B.; Phillips, R. J. *Coord. Chem. Rev.* **1980**, *33*, 227.

(39) Hathaway, B. J. In *Comprehensive Coordination Chemistry*; Wilkinson, R. D., Gill, J. A., Eds.; McCleverty, Pergamon Press: Oxford, 1987; Vol. 5.

(40) (a) Boudroux, E. A.; Mulay, L. N. *Theory and Applications of Molecular Paramagnetism*; John Wiley: New York, 1976. (b) Brown, D. B.; Wasson, J. R.; Hall, J. W.; Hatfield, W. E. *Inorg. Chem.* **1977**, *16*, 2526.

Table 3. Selected Bond Lengths (Å) and Angles (deg) for $[Cu_3(L)_2(CH_3COO)_2(OH)_2(dmf)_2]$[a]

Cu(1)−O(1)	1.891(2)	Cu(2)−O(1)#1	1.902(2)
Cu(1)−O(21)	1.980(2)	Cu(2)−O(1)	1.902(2)
Cu(1)−N(2)	1.997(3)	Cu(2)−O(22)#1	1.968(2)
Cu(1)−N(1)	2.005(3)	Cu(2)−O(22)	1.968(2)
Cu(1)−O(30)	2.517(4)	Cu(2)−O(30)#1	2.703(5)
Cu(1)−Cu(2)	3.1983(4)	Cu(2)−O(30)	2.703(5)
O(1)−Cu(1)−O(21)	90.55(9)	O(1)#1−Cu(2)−O(22)	88.12(10)
O(1)−Cu(1)−N(2)	99.42(10)	O(1)−Cu(2)−O(22)	91.88(10)
O(21)−Cu(1)−N(2)	161.53(10)	O(22)#1−Cu(2)−O(22)	180.0
O(1)−Cu(1)−N(1)	175.92(10)	O(1)#1−Cu(2)−O(30)#1	78.15(11)
O(21)−Cu(1)−N(1)	87.40(9)	O(1)−Cu(2)−O(30)#1	101.85(11)
N(2)−Cu(1)−N(1)	81.62(11)	O(22)#1−Cu(2)−O(30)#1	86.14(11)
O(1)−Cu(1)−O(30)	83.41(15)	O(22)−Cu(2)−O(30)#1	93.86(11)
O(21)−Cu(1)−O(30)	88.12(12)	O(1)#1−Cu(2)−O(30)	101.85(11)
N(2)−Cu(1)−O(30)	108.33(12)	O(1)−Cu(2)−O(30)	78.15(11)
N(1)−Cu(1)−O(30)	100.05(15)	O(22)#1−Cu(2)−O(30)	93.86(11)
O(1)#1−Cu(2)−O(1)	180.0	O(22)−Cu(2)−O(30)	86.14(11)
O(1)#1−Cu(2)−O(22)#1	91.88(10)	O(30)#1−Cu(2)−O(30)	180.0
O(1)−Cu(2)−O(22)#1	88.12(10)	Cu(1)−O(1)−Cu(2)	114.96(12)

[a] Symmetry transformations used to generate equivalent atoms: #1, $-x + 1, -y, -z + 1$.

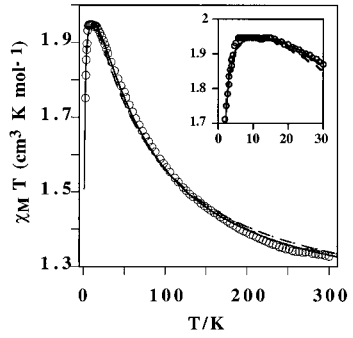

Figure 2. Temperature dependence of $\chi_M T$ for $[Cu_3(L)_2(CH_3COO)_2(OH)_2(dmf)_2]$. The solid and broken lines represent the fitted functions as described in the text.

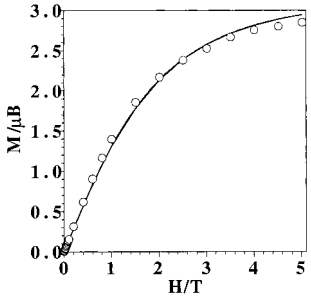

Figure 3. Field dependence of magnetization for $[Cu_3(L)_2(CH_3COO)_2(OH)_2(dmf)_2]$ at 2 K.

curves for different J and J' values, ranging from 80 to 100 cm^{-1} and from +10 to −10 cm^{-1}, respectively, for $g \approx 2.06$ (R values ranging from 1×10^{-5} to 1×10^{-4}, $R = \sum_i[(\chi_M T)_{obsd,i} - (\chi_M T)_{calcd,i}]^2/\sum_i[(\chi_M T)_{obsd,i}]^2$. The fitting to the experimental data including the low-temperature region where D is operative shows a similar correlation between J and J'. The solid and broken lines in Figure 2 represent typical fits with $J = 87$ cm^{-1}, $J' = 0$ (fixed), $|D| = 1.61$ cm^{-1}, $g = 2.05$, and $R = 3 \times 10^{-5}$ and $J = 99$ cm^{-1}, $J' = -10$ cm^{-1}, $|D| = 1.62$ cm^{-1}, $g = 2.05$, and $R = 8 \times 10^{-5}$, respectively. Consequently, $J = 93(6)$ cm^{-1} and $J' = -5(5)$ cm^{-1}. These J and J' values are indicative of a strong ferromagnetic coupling and a weak antiferromagnetic one.

The field dependence of the magnetization $M = f(H)$ measured at 2 K is given in Figure 3. The magnetization varies linearly with low applied fields up to ca. 0.6 T and then progressively tends to saturation. The variation of M with H does not follow that predicted by the Brillouin function for $S = 3/2$ with $g = 2.05$ in the case of a normal Curie-law system. When zero-field splitting occurs, magnetization becomes anisotropic due to the different populations of the components of the zero-field-split ground state as the orientation of the magnetic field is varied with respect to the molecule. Consequently, to simulate the M vs H curve, it is necessary to evaluate the average of M for all orientations.[41] Taking this fact into account, we have simulated the magnetic data with a full-matrix diagonalization routine using the Hamiltonian $\mathbf{H} = D[\mathbf{S_z}^2 - (1/3)S(S + 1)] + g\beta H\mathbf{S_z}$ for $S = 3/2$ with the calculated $|D| = 1.61$ cm^{-1} and $g = 2.05$ values. A reasonably good agreement between experimental and calculated M data is achieved, as observed in Figure 3.

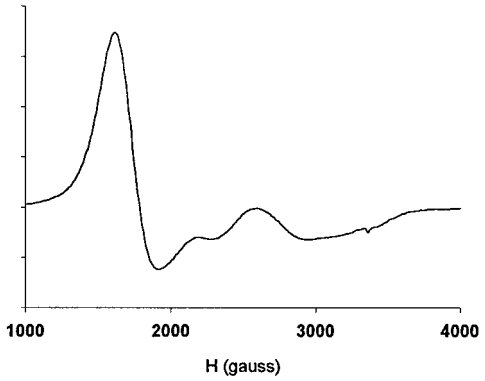

Figure 4. Polycrystalline powder EPR spectrum of $[Cu_3(L)_2(CH_3COO)_2(OH)_2(dmf)_2]$ at 40 K.

EPR Spectrum. The polycrystalline powder X-band EPR spectrum of the title complex at 40 K (Figure 4) is dominated by a transition at 1606 G which unambiguously identifies the spin of the ground multiplet ($S = 3/2$). Since from the magnetic data the observed energy gap between the ±1/2 and ±3/2 Kramers doublets, $|2D| = 3.2$ cm^{-1}, is much greater than $h\nu = 0.31$ cm^{-1} (where ν is the spectrometer frequency), only the signals within the ±1/2 and ±3/2 Kramers doublets can be observed. Furthermore, variable-temperature studies reveal that the intensity of the $M_s = \pm 1/2$ EPR spectrum increases with decreasing temperature (Figure 5), showing that the $M_s = \pm 1/2$ levels are the ground state. Consequently, only transitions within the $M_s = \pm 1/2$ doublet with an effective $S' = 1/2$ Hamiltonian are observed. At 4 K the effective values g_x' and g_y' found at 4.25 can be assigned to the transition between ±1/2 levels of the $S = 3/2$ system. The corresponding weaker g_z' signal, expected to be close to 2.0, is not observed.

(41) (a) Boyd, P. D. W.; Martin, R. L. *J. Chem. Soc., Dalton Trans.* **1979**, 92. (b) Gerloch, M.; Meeking, R. F. *J. Chem. Soc., Dalton Trans.* **1975**, 2443.

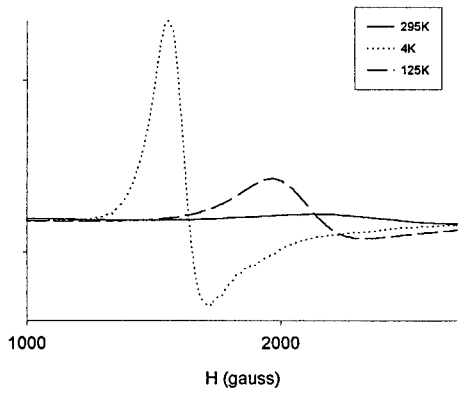

Figure 5. X-band powder EPR spectra of $[Cu_3(L)_2(CH_3COO)_2(OH)_2(dmf)_2]$.

In the case of an axial symmetry, it has been shown that the observed g' values of the effective $S' = 1/2$ state are related to the true values of the $S = 3/2$ state by the following relations:[10]

$$g'_{\parallel} = g_{\parallel} \quad \text{and} \quad g_{\perp}' = 2g_{\perp}$$

where $g_{\parallel}$ and $g_{\perp}$ are the true Zeeman parameters of the quartet state. In our case, $g_{\perp}' = 4.25$ and $g_{\perp} = 2.12$. As the g_{av} value obtained from the magnetic measurements is 2.05, the true $g_{\parallel}$ value estimated is around 2.00.

Rising temperature leads to a strong shift of the resonance at 1585 G (4 K) toward higher fields (Figure 5). At room temperature a broad signal at $g \approx 3.16$ was detected. This fact has also been observed in the (octachlorodiadeniniumtricopper-(II) linear trinuclear Cu(II) complex,[42] where a variation of g between 4.2 and 300 K on the order of $\Delta g \approx 0.03$ was reported. Variations of the thermal population of different spin levels were assumed to explain this effect. Haase et al.[10] have detected the same phenomenon with a $\Delta g \approx 1.7$. Following the Haase et al. analysis of the thermal dependence of the g value, a least-squares fit of eq 5 to the experimental data varying the energy separation

$$H_{\text{res,calcd}} = \frac{\sum \varpi H_{\text{res},i} \exp\{-\Delta E_i/kT\}}{\sum \varpi \exp\{-\Delta E_i/kT\}} \qquad (5)$$

between the spin doublet levels was carried out. $H_{\text{res},i}$ is the resonance field, ϖ is the multiplicity, and ΔE_i is the energy separation observed in Chart 2.

Taking into account the resonance field at 1585 G of the $S' = 1/2$ state from the EPR spectra at 4 K, the best fit was obtained for $\Delta E_1 = 46$ cm^{-1}, $\Delta E_2 = 147$ cm^{-1}, $H_{\text{res},1} = 2949$ G ($g = 2.30$), and $H_{\text{res},2} = 3140$ G ($g = 2.16$). These parameters correspond to $J = 98$ cm^{-1} and $J' = -3$ cm^{-1}.

The calculated curve and the experimental resonance fields are shown in Figure 6. The reasonably good agreement between the obtained parameters ΔE_1 and ΔE_2 and those obtained from the magnetic measurements proves the above-mentioned hypothesis that the strong g shift is due to a temperature-dependent contribution of the resonance fields of the three spin states to a composed EPR signal.

Ferromagnetic Exchange Interaction. In the case of dinuclear copper(II) complexes, it is well-known that *syn*−*syn* carboxylato bridges and hydroxo bridges, with an angle at the hydroxo bridge larger than 97.5°, cause antiferromagnetic coupling.[18,43] Consequently, the expected magnetic coupling in

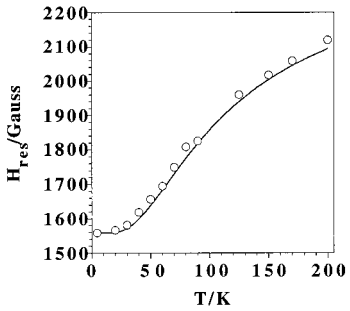

Figure 6. Temperature dependence of the resonance fields of $[Cu_3(L)_2(CH_3COO)_2(OH)_2(dmf)_2]$.

$[Cu_3(L)_2(CH_3COO)_2(OH)_2(dmf)_2]$ should be antiferromagnetic. However, when the bridging ligands are different, the two bridges may either add or counterbalance their effects. This problem was treated by Nishida et al.,[44−46] Mckee et al.,[47,48] and one of us,[49] these phenomena being known as orbital complementarity and countercomplementarity, respectively. In the present case, the antiferromagnetic contributions of each bridge almost cancel each other out (i.e., these bridges exhibit an orbital countercomplementarity) and the ferromagnetic term dominates ($J_T = J_{AF} + J_F$, with $|J_{AF}|$ being smaller than $|J_F|$).

To show the concurrence of this phenomenon in $[Cu_3(L)_2(CH_3COO)_2(OH)_2(dmf)_2]$, we have used Hoffman's approach,[50] in which the magnitude of the antiferromagnetic term (J_{AF}) is considered to be proportional to the square of the energy gap (Δ) between the two singly occupied molecular orbitals (SOMOs). The value of Δ has been computed through MO calculations on the triplet state, which are based on the density-functional theory (DFT).[19] At the same time, we have calculated the exchange coupling constant using the broken-symmetry approach. In the complex a hydroxo bridge and a carboxylato bridge connect, two at a time, the three copper(II) magnetic orbitals. This bridging arrangement is shown in the model dinuclear copper(II) system III (Chart 3), in which the hydroxo bridging angle was fixed at 114.9° and the other structural parameters (bond angles and distances) were averaged from the experimental ones. With the aim of analyzing independently the role of each bridging unit, we also performed DFT calculations on models I and II shown in Chart 3. In these models, the hydroxo bridge and carboxylato bridge, respectively, have been replaced by two ammonia molecules. To avoid the ammonia contacts, a rotation has been carried out to prevent a perpendicular disposition of the basal plane with respect to the bridging ligand plane.

The results of the calculations are illustrated in Figure 7. The in-phase and out-of-phase combinations of the metal orbitals ($d_{x^2-y^2} \pm d_{x^2-y^2}$) interact with the symmetry-adapted HOMOs of the bridging ligand carboxylate or hydroxo to give the corresponding SOMOs φ^S and φ^{AS} and φ'^S and φ'^{AS}, respectively. The superscripts AS and S refer to antisymmetric and

(42) Banci, L.; Bencini, A.; Gatteschi, D. *Inorg. Chem.* **1983**, *22*, 2681.
(43) Lewis, D. L.; NcGregor, K. T.; Hogson, W. E.; Hodgson, D. J. *Inorg. Chem.* **1974**, *13*, 147.
(44) Nishida, Y.; Kida, S. *J. Chem. Soc., Dalton Trans.* **1986**, 2633.
(45) Nishida, Y.; Takeuchi, M.; Takahashi, K.; Kida, S. *Chem. Lett.* **1985**, 631.
(46) Nishida, Y.; Takeuchi, M.; Takahashi, K.; Kida, S. *Chem. Lett*. **1983**, 1815.
(47) McKee, V.; Zvagulis, M.; Reed, C. A. *Inorg. Chem.* **1985**, *24*, 2914.
(48) McKee, V.; Zvagulis, M.; Dagdian, J. V.; Patch, M. G.; Reed, C. A. *J. Am. Chem. Soc.* **1984**, *106*, 4765.
(49) Thompson, L. K.; Tandon, S. S.; Lloret, F.; Cano, J.; Julve, M. *Inorg. Chem.* **1997**, *36*, 3301.
(50) Hay, P. J.; Thibeault, J. C.; Hoffmann, R. *J.Am. Chem. Soc.* **1975**, *97*, 4884.

Chart 3. Dinuclear Cu(II) Models for DFT Calculations

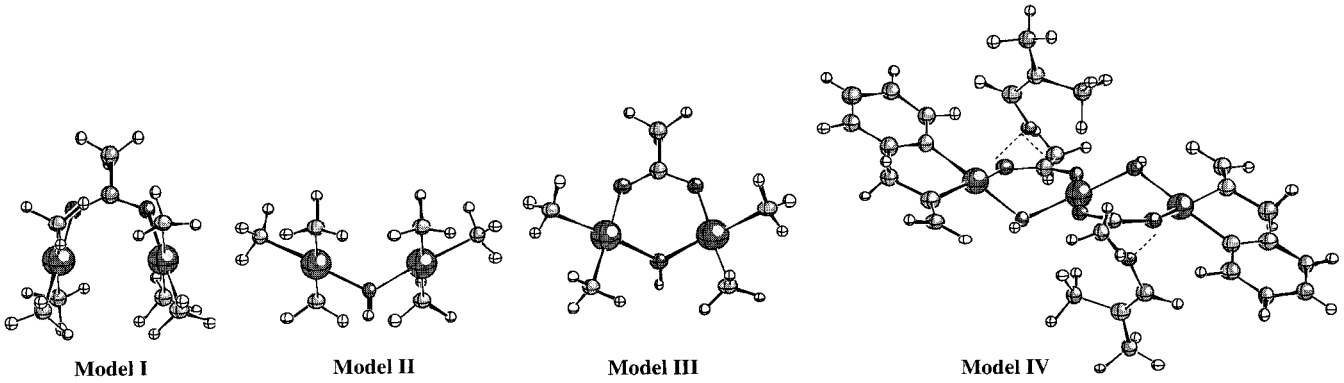

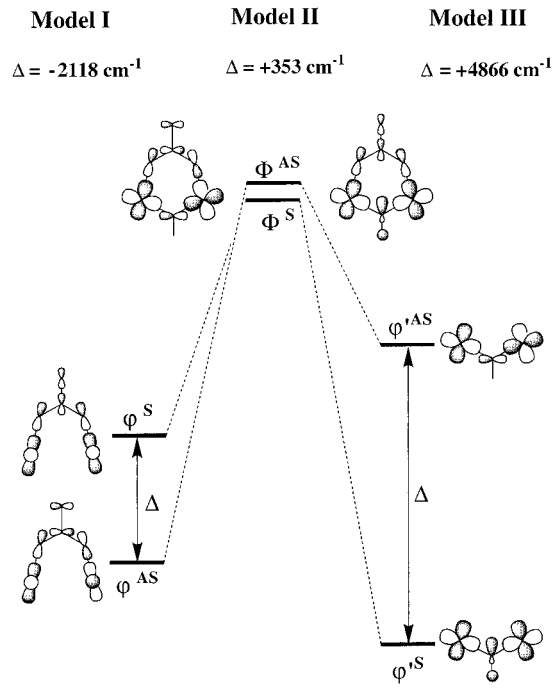

Figure 7. MO diagram for a model dinuclear copper(II) unit with a μ-carboxylato bridge (model I), a μ-hydroxo bridge (model II), and both bridging ligands (model III).

symmetric character with respect to the mirror plane perpendicular to the molecular plane of the models. The energy gap, $\Delta = E_{AS} - E_S$, in both cases is important and in agreement with the antiferromagnetic coupling observed in complexes where only one of these bridges is present and with the calculated exchange coupling constants ($J = -44$ and -219 cm^{-1} for models I and II, respectively. In model I (absence of the hydroxo bridge) the higher SOMO is the symmetric φ^S, whereas in model II (the absence of the carboxylato bridge) the higher SOMO is the antisymmetric φ'^{AS}. This is the reason for the difference in the sign of Δ (-2118 and $+4866$ cm^{-1}) in these two cases, and it is the origin of the countercomplementarity of the two bridges. Therefore, when we consider the simultaneous presence of both bridges in model III (Chart 3), the difference in energy (Δ) of the SOMOs Φ^{AS} and Φ^S ($+353$ cm^{-1}) is very small, and so the resulting antiferromagnetic term would be very small, leading to a situation where the ferromagnetic term would become dominant, which is exactly the situation observed for $[Cu_3(L)_2(CH_3COO)_2(OH)_2(dmf)_2]$.

Finally, we have calculated the exchange coupling constants for a model of our trimer compound (model IV), where we have simplified only the more external part of the terminal ligands, keeping experimental positions for the remaining atoms, including the solvate molecules. In this way, there should be no changes due to the modelization of the J values. We have obtained important ferromagnetic ($J = 120$ cm^{-1}) and weak antiferromagnetic ($J' = -32$ cm^{-1}) interactions between neighboring and nonneighboring centers, respectively. The calculated value of J is in agreement in nature and magnitude with the experimental value ($J = 93(6)$ cm^{-1}). The small discrepancies are attributed to the effects of the modelization and the possibility to find different good experimental fits.

In a previous paper Haase et al.[10d] have investigated the exchange coupling in a series of mixed-bridged μ-alcoxo, μ-carboxylato trinuclear compounds leading to a quartet ground state with J ranging in the region $50-70$ cm^{-1}. Interestingly, the mixed-bridged moieties Cu(1)$-$RO/RCO$_2-$Cu(2) retain their structural properties independent from the Cu_3 symmetry. No influence on the exchange coupling between adjacent centers was found when the Cu_3 unit was linear or angular. In addition, they have pointed out that the folding angle φ, defined by the two planes where the Cu(1) and Cu(2) atoms lie, is correlated with the angle ϕ (Cu(1)$-$O(1)$-$Cu(2)) in such a way that the greater the φ the smaller the ϕ observed. From SCF-CI calculations based on a dimeric model, these authors have also shown the occurrence of a ferromagnetic coupling and a J_{calcd} almost constant in the range $50° \leq \varphi \leq 70°$ in agreement with their experimental results.

Our DFT calculations based on the trinuclear model together with our experimental results show an excellent agreement with the magnetostructural correlations deduced by Haase et al. Finally, it should be pointed out that $[Cu_3(L)_2(CH_3COO)_2(OH)_2(dmf)_2]$ illustrates dramatically the countercomplementary effect imposed by the carboxylato bridge, which attenuates the effect of the antiferromagnetic hydroxo bridge to the point where strong ferromagnetic behavior is observed. The choice of bridges exhibiting orbital countercomplementarity could be used in the synthesis of high-spin molecules or materials which may exhibit enhanced spontaneous bulk magnetic ordering.

Acknowledgment. G.A. and J.B. thank CYCIT (Project PM97-0105-C02-01), A.C. thanks the Xunta de Galicia (Project XUGA20309B97), and J.A.R. thanks CYCIT (Project PB97-1397) and the TMR European Community (Contract ERBFMRXCT-980181) for financial support.

Supporting Information Available: Tables listing detailed crystallographic data, atomic positional parameters, anisotropic thermal parameters, bond lengths and angles, and least-squares planes. This material is available free of charge via the Internet at http://pubs.acs.org.

IC000218M